Research Square

Preprints are preliminary reports that have not undergone peer review.
They should not be considered conclusive, used to inform clinical practice,
or referenced by the media as validated information.

Construction of a Risk Stratification Model for Severe Mycoplasma pneumoniae Pneumonia in Children Based on PRDM1, LDH, CRP, and the PRESS Score

Mingjing Jiang
Zunyi Medical University
Aiping Wei
Zunyi Medical University
Jiayan Dong
Zunyi Medical University
Yuanhang Ai
Zunyi Medical University
Longying Liang
Zunyi Medical University
Tingting Li
Zunyi Medical University
Kaifeng Wu
Zunyi Medical University
Shifei Yao
shifeiyao1005@163.com
Zunyi Medical University

Research Article

Keywords: severe Mycoplasma pneumoniae pneumonia, children, immune biomarkers, PR domain zinc finger protein 1, nomogram

Posted Date: November 11th, 2026

DOI: https://doi.org/10.21203/rs.3.rs-11026292/v1

License: This work is licensed under a Creative Commons Attribution 4.0 International License.
Read Full License

Additional Declarations: No competing interests reported.

Construction of a Risk Stratification Model for Severe *Mycoplasma pneumoniae* Pneumonia in Children Based on PRDM1, LDH, CRP, and the PRESS Score

Mingjing Jiang[a], Aiping Wei[a],Jiayan Dong[a], Yuanhang Ai[a], Longying Liang [a], Tingting Li [a], Kaifeng Wu[a, b#], Shifei Yao[a, #]

[a] Department of Laboratory Medicine, The Third Affiliated Hospital of Zunyi Medical University (The First People's Hospital of Zunyi), Zunyi 563000, Guizhou Province, China.

[b] Scientific Research Center, The Third Affiliated Hospital of Zunyi Medical University (The First People's Hospital of Zunyi), Zunyi 563000, Guizhou Province, China.

[#] **Correspondence:**

Kaifeng Wu, Department of Laboratory Medicine, The Third Affiliated Hospital of Zunyi Medical University (The First People's Hospital of Zunyi), Zunyi 563000, Guizhou Province, China; E-mail: kiphoonwu@zmu.edu.cn.

Shifei Yao, Department of Laboratory Medicine, The Third Affiliated Hospital of Zunyi Medical University (The First People's Hospital of Zunyi), Zunyi 563000, Guizhou Province, China; E-mail: shifeiyao1005@163.com.

Abstract

Background: Severe *Mycoplasma pneumoniae* pneumonia (SMPP) leads to poor outcomes in children, while reliable early risk stratification tools are currently insufficient. This study constructed and internally evaluated an SMPP risk stratification model combining novel immune biomarkers and routine laboratory indicators to support early risk identification and individualized clinical management of pediatric SMPP.

Methods: This retrospective single-center study enrolled 235 hospitalized children with MPP (164 mild and 71 severe cases) and 40 healthy controls from October 2023 to January 2026. Candidate immune biomarkers were screened based on published single-cell transcriptomic datasets and validated via RT-qPCR and ELISA. We applied LASSO-logistic regression and multivariable analysis to screen independent SMPP risk determinants, using validated immune biomarkers, clinical data, laboratory parameters and disease severity scores as candidate predictors. A nomogram-based risk stratification model was subsequently constructed. The MPP cohort was randomly split into training and test sets at a 7:3 ratio. Model performance was comprehensively assessed via ROC curve, Bootstrap calibration curves, and decision curve analysis (DCA).

Results: PBMC-derived PRDM1 mRNA and serum PRDM1 protein levels were significantly elevated in children with SMPP ($P < 0.05$), indicating aberrant PRDM1 expression in severe pediatric MPP. Four independent risk determinants were screened, including the PRESS score, LDH, CRP, and serum PRDM1. The nomogram showed excellent discriminatory ability, with AUCs of 0.924 (95% CI: 0.881-0.967) for the training set and 0.856 (95% CI: 0.751–0.962) for the test set. The model exhibited good calibration (training MAE = 0.050; testing MAE = 0.036), and DCA showed sustained clinical net benefit across threshold probability range of 0.02-0.85.

Conclusions: This nomogram-based risk stratification model integrating PRDM1, PRESS score,

LDH and CRP, possesses good discrimination, favorable calibration and reliable clinical utility. It facilitates early risk assessment and standardized stratified management for pediatric SMPP and aids precise clinical decision-making.

Keywords: severe *Mycoplasma pneumoniae* pneumonia; children; immune biomarkers; PR domain zinc finger protein 1; nomogram**.**

1. Background

Mycoplasma pneumoniae (MP) is a dominant pathogen of pediatric lower respiratory tract infections in children aged over 5 years in China[1]. MP outbreaks follow a periodic cycle, with national epidemic emerging every 3-7 years[2]. During epidemic surges, hospital admissions for *Mycoplasma pneumoniae* pneumonia (MPP) rise sharply and impose heavy strain on primary and tertiary healthcare systems[3]. While standard antimicrobial therapy yields favorable outcomes for most children with uncomplicated MPP, a subset rapidly deteriorates into severe *Mycoplasma pneumoniae* pneumonia (SMPP). SMPP manifests as persistent high fever, progressive dyspnea, extensive pulmonary infiltrates and extra-pulmonary complications， which may culminate in permanent pulmonary sequelae or fatal deterioration in critical cases. [4-6].

Current clinical screening for SMPP relies primarily on clinical identification, chest radiography and routine biomarkers including C-reactive protein (CRP), lactate dehydrogenase (LDH), and D-dimer[1]. Nevertheless, these markers are susceptible to confounding factors such as disease phase, sampling timing, coinfections and comorbidities, compromising their specificity for early risk discrimination. Repeated chest computed tomography also exposes children to cumulative ionizing radiation, further limiting its frequent clinical application[7, 8]. Accordingly,

timely and accurate identification of children prone to severe MPP remains an unmet clinical need for standardized diagnosis, intervention and risk-stratified management.

The pathogenesis of MPP is driven not only by direct MP invasion but also by aberrant host immune-inflammatory responses, which are key contributors to disease aggravation[9]. MP infection activates both innate and adaptive immunity, balanced immune activation facilitates pathogen elimination, whereas disrupted immune homeostasis triggers a massive cytokine storm, aberrant immune cell activation and systemic tissue damage, accelerating progression from mild MPP to SMPP [10, 11]. Previous studies have shown that dysregulated cytokines such as IL-6, IL-10, IFN-γ, IL-17A and altered peripheral immune cell populations correlate closely with MPP severity[11-14]. These findings indicate that immune dysregulation is closely involved in the progression of MPP and may provide complementary information beyond conventional clinical and laboratory indicators, thereby supporting the incorporation of immune biomarkers into SMPP risk stratification.

Despite these immunological insights, existing models for severe or refractory MPP have been constructed mainly based on clinical phenotypes, routine laboratory tests, and imaging parameters[15-17]. These conventional indicators primarily capture macroscopic phenotypic alterations that occur secondary to disease progression, yet fail to characterize the underlying immune dysregulation associated with SMPP progression. Integration of specific immune biomarkers may compensate for this deficiency by providing molecular-level immune signatures unobtainable from routine clinical parameters, thereby improving the comprehensiveness and accuracy of current SMPP risk stratification systems.

Single-cell RNA sequencing (scRNA-seq) profiles immune cell composition, subset distribution, and functional states at single-cell resolution, serving as a powerful tool to dissect

heterogeneous immune responses across children with MPP of varying severity. Prior scRNA-seq profiling of bronchoalveolar lavage fluid specimens from pediatric mild and severe MPP patients uncovered divergent local immune landscapes, implicating T-cell exhaustion, cellular apoptosis and inflammatory dysregulation as core mechanisms driving SMPP pathogenesis. Leveraging the public transcriptomic dataset OMIX007208[10], we first screened candidate immune genes associated with SMPP severity. We further validated transcriptional expression of target genes via RT-qPCR and their circulating protein concentrations in serum via ELISA, and quantified their correlations with MPP severity. Combining validated immune biomarkers, baseline clinical data, routine laboratory readouts and the Pediatric Respiratory Severity Score (PRESS), we constructed an SMPP risk stratification model. This study ultimately seeks to deliver a quantitative reference for early screening and tiered clinical management of children at high risk of progressing to SMPP.

2. Methods

2.1 Study Design and Ethics

This single-center retrospective observational study was performed following the ethical guidelines outlined in the Declaration of Helsinki and all subsequent revisions. The study protocol received ethical approval from the Ethics Committee of Zunyi First People's Hospital on September 6, 2023 (Approval No. Ethics Review [2023]-1-271). Written informed consent was collected from the parents or legal guardians of all enrolled subjects.

2.2 Study Population

This retrospective study consecutively enrolled hospitalized children diagnosed with MPP who were admitted to the Department of Pediatrics, the First People's Hospital of Zunyi, from October 2023 to January 2026. Age distribution-matched children aged under 18 years receiving routine physical examinations over the same period were recruited as healthy controls (HCs). The

HC cohort was only adopted to compare the expression profiles of immune biomarker and was not incorporated into the construction of the risk stratification model. This design eliminating non-disease-related confounding variables that might compromise model stability.

Inclusion criteria: All MPP patients were diagnosed strictly in accordance with the *Guideline for the Diagnosis and Treatment of Mycoplasma pneumoniae Pneumonia in Children (2023 Edition)*[1]. A definitive MPP diagnostic required typical clinical manifestations and characteristic radiographic abnormalities, accompanied by confirmatory laboratory evidence of MP infection, which satisfied either of the following criteria: (a) a single serum MP particle agglutination antibody titer $\geqslant$1:160, or a $\geqslant$4-fold rise in paired acute-phase and convalescent serum MP antibody titers; (b) positive MP-DNA or MP-RNA results from respiratory specimens.

Healthy controls were age-matched children under 18 years old who met all of the following requirements: absence of any systemic infectious manifestations; no exposure to antibiotics, corticosteroids, or immunomodulators within two weeks prior to enrollment; and no preexisting diseases disrupting immune and inflammatory homeostasis.

Exclusion criteria: Subjects satisfying any of the following conditions were excluded from this study: (1) receiving continuous immunosuppressive therapy or diagnosed with congenital or acquired immunodeficiency disorders; (2) microbiologically confirmed coinfection with bacteria, fungi, viruses, or other atypical pathogens before or during hospitalization; (3) symptom duration $\geqslant$7 days on initial hospital admission; (4) incomplete clinical, laboratory, or imaging data that precluded valid statistical analysis; (5) preexisting comorbidities that could disrupt systemic inflammatory responses, coagulation function, or function of vital organs.

Severity classification: SMPP was defined based on the 2023 pediatric MPP clinical guideline[1]. Patients were diagnosed with SMPP if they met one or more of the following

standards: (1) persistent high fever (body temperature ≥39 °C) lasting no less than 5 days, or prolonged fever (⩾7 days) with sustained peak fever temperature or recurrent febrile episodes; (2) respiratory manifestations including wheezing, tachypnea, dyspnea, chest pain or hemoptysis, accompanied by extensive pulmonary lesion, plastic bronchitis, acute asthma exacerbation, pleural effusion, or pulmonary embolism; (3) the presence of extrapulmonary organ involvement that did not fulfill the diagnostic criteria for critical illness; (4) resting pulse oxygen saturation ≤0.93 measured at sea level under room-air conditions; (5) severe radiographic manifestations, including any one of the following: (a) dense pulmonary consolidation involving two-thirds or more of a single lobe, or dense consolidation involving two or more lobes regardless of lesion scope; (b) unilateral or bilateral diffuse bronchiolitis, which may be accompanied by bronchitis, bronchial wall thickening, peribronchial exudation, mucus plug formation, and secondary atelectasis; (6) progressive clinical deterioration with radiologically confirmed lesion enlargement exceeding 50% within 24 to 48 hours; (7) markedly elevated levels of CRP, LDH, or D-dimer.

2.3 Clinical Data Collection and Sample Processing

Baseline demographic data, clinical manifestations, chest radiographic results, and laboratory indicators were recorded for all enrolled MPP patients at admission. In admission, PRESS scores and modified PIRO (mPIRO) scores were calculated and documented [18, 19]. Peripheral venous blood samples were collected at admission and processed immediately.

All blood specimens obtained from both patients and healthy controls were processed on-site immediately after collection. Briefly, serum was separated, aliquoted, and stored at −80 °C. PBMCs were isolated by Ficoll density-gradient centrifugation, lysed with TRIzol reagent, and preserved at −80 °C for downstream experiments.

2.4 Candidate Immune Biomarker Selection and Measurement

Based on previously published single-cell transcriptomic profiling data comparing children with mild and severe MPP[10], eleven immune-related candidate genes were screened and classified into four major functional modules: T-cell exhaustion (*PDCD1*, *CTLA4*, *HAVCR2*, *LAG3*), immune regulation (*PRDM1*, *PTPN6*, *IDO1*), apoptosis (*TNFSF10*), and inflammatory activation (*IL1B*, *CXCL8*, *S100A8*). Total RNA was extracted from PBMCs and reverse-transcribed into complementary DNA. The mRNA expression of all candidate genes was detected via real-time quantitative polymerase chain reaction (RT-qPCR). Glyceraldehyde-3-phosphate dehydrogenase (*GAPDH*) was applied as an endogenous reference gene, and the $2^{-\Delta\Delta Ct}$ method was applied to calculate relative gene expression. Primer sequences for RT-qPCR are provided in Supplementary Table S1 (Additional file).

For genes exhibiting significant transcriptional intergroup differences, the serum concentrations of their encoded proteins (S100A8, PRDM1, and TNFSF10) were further measured using commercial ELISA kits. The S100A8 kit (Cat. No. FY-EH2668) was obtained from Feiyue Biotechnology Co., Ltd.,China; the PRDM1 kit (Cat. No. MM-64065H1) was supplied by Meimian Biotechnology Co., Ltd. China; and the TNFSF10 kit (Cat. No. JL1391) was purchased from Jianglai Biotechnology Co., Ltd. China. All ELISA procedures were performed strictly following the manufacturers' instructions.

2.5 Model Construction and Evaluation

A random seed of 42 was set to ensure reproducibility, and children with MPP were randomly split into training and test cohorts at a 7:3 ratio. Candidate variables included admission clinical characteristics, routine laboratory indicators, and serum immune biomarkers. Variables with missing proportions exceeding 30% were directly excluded, and the remaining missing data were imputed via the MissForest algorithm[20]. Continuous variables were standardized with Z-score transformation before LASSO penalization to stabilize coefficient shrinkage; the final risk stratification model was constructed using raw unstandardized data to guarantee clinical interpretability of odds ratios. 10-fold cross-validation was implemented on the training cohort to screen indicators based on the λ.min and λ.1se criteria[21]. Indicators retained at the λ.min threshold were further incorporated into multivariable logistic regression. All candidate risk stratification models were compared in terms of discriminative performance and clinical interpretability, and a visualized risk stratification nomogram was established based on the optimal model.

Model performance was assessed in both training and test cohorts. Discriminative capacity for risk grouping was quantified via ROC curves and AUC[22]. Calibration was visualized using calibration curves generated from 1000 bootstrap resamples, with MAE calculated for quantitative calibration assessment[23]. DCA was applied to evaluate the clinical net benefit of this risk stratification tool [24]. A two-sided $P < 0.05$ was defined as the threshold for statistical significance.

2.6 Statistical Analysis

All statistical analyses were conducted using SPSS version 29.0 and the Deepwise & Beckman Coulter DxAI platform. SPSS 29.0 was used for baseline descriptive statistics and

between-group comparative analyses, whereas model construction and evaluation, including LASSO-logistic regression, multivariable logistic regression, nomogram construction, ROC analysis, calibration assessment, and decision curve analysis, were performed using the Deepwise & Beckman Coulter DxAI platform.

Normally distributed continuous variables were reported as mean ± standard deviation and compared via the independent samples t-test or one-way analysis of variance (ANOVA). Non-normally distributed continuous variables were presented as median with interquartile range [M (Q1, Q3)] and compared using the Mann–Whitney U test or Kruskal–Walli's test, as appropriate. Categorical variables are expressed as counts and proportions [n (%)], with between-group differences assessed using the χ^2 test or Fisher's exact test when applicable. All statistical tests were two-sided, and $P < 0.05$ was defined as the threshold for statistical significance.

3. Results

3.1 Baseline Characteristics of the Study Population

A total of 275 subjects were enrolled in this study, consisting of 235 children with MPP (164 mild cases and 71 severe cases) and 40 healthy controls. Only the baseline clinical manifestations and laboratory parameters of MPP patients were compared between the mild and severe subgroups, healthy controls were not included in this comparison, and the data are summarized in Table 1. Compared with children in the mild subgroup, patients with SMPP exhibited significantly elevated heart rate, respiratory frequency, LDH, CRP, PRESS score, and mPIRO score ($P < 0.05$). In contrast, the severe subgroup presented younger age, lower body weight, and significantly reduced levels of prealbumin, total protein, cholinesterase, alkaline phosphatase, creatinine, and hematocrit ($P < 0.05$). Complete between-group comparisons are provided in Supplementary Tables S2–S6 (Additional file 1).

Table 1. Comparison of Baseline Clinical and Laboratory Characteristics Between the Mild and Severe Groups

Variable	Mild Group (n = 164)	Severe Group (n = 71)	*P*
Heart rate (beats/min)	109.0 [102.0, 120.5]	124.0 [108.0, 133.0]	<0.001
Respiratory rate (breaths/min)	26.0 [23.0, 30.0]	33.0 [28.0, 37.0]	<0.001
Age (months)	70.0 [48.0, 88.5]	48.0 [30.0, 75.0]	<0.001
Body weight (kg)	19.0 [15.0, 25.0]	17.0 [13.8, 21.0]	0.003
LDH (U/L)	282.0 [251.0, 309.0]	321.0 [281.0, 377.0]	<0.001
CRP (mg/L)	3.93 [1.09, 10.61]	6.91 [2.70, 16.73]	0.009
Prealbumin (mg/L)	145.9 [125.0, 180.1]	118.2 [101.7, 146.1]	<0.001
Total protein (g/L)	70.3 [67.0, 72.0]	66.7 [64.3, 69.2]	0.001
Cholinesterase (U/L)	8698.0 [7839.0, 9351.0]	7413.0 [6702.0, 8213.0]	<0.001
Alkaline phosphatase (U/L)	213.0 [178.0, 246.0]	188.0 [157.0, 224.0]	0.019
Creatinine (μmol/L)	34.1 [29.8, 41.0]	29.8 [26.3, 34.2]	<0.001
Hematocrit (%)	38.3 [37.0, 40.6]	37.9 [35.7, 39.7]	0.036
PRESS score (points)	0.0 [0.0, 0.0]	1.0 [0.0, 2.0]	<0.001
mPIRO score (points)	0.0 [0.0, 1.0]	1.0 [0.0, 1.0]	<0.001

Note: Continuous variables are presented as median [P25, P75]. LDH: lactate dehydrogenase; CRP: C-reactive protein; PRESS: Pediatric Respiratory Severity Score; mPIRO: modified PIRO score.

3.2 Screening and Validation of Candidate Immune Biomarkers

To verify the candidate immune-related genes screened from prior single-cell transcriptomic data, RT-qPCR was performed to quantify the mRNA expression of 11 target genes in PBMCs isolated from peripheral blood specimens of MPP children. The results revealed that the mRNA levels of *PRDM1*, *S100A8*, and *TNFSF10* in PBMCs were markedly upregulated in the severe subgroup compared with the mild subgroup ($P < 0.05$). No significant intergroup differences were observed for the other eight genes (*PDCD1*, *CTLA4*, *HAVCR2*, *LAG3*, *IDO1*, *PTPN6*, *IL1B*, and *CXCL8*) (Figure 1).

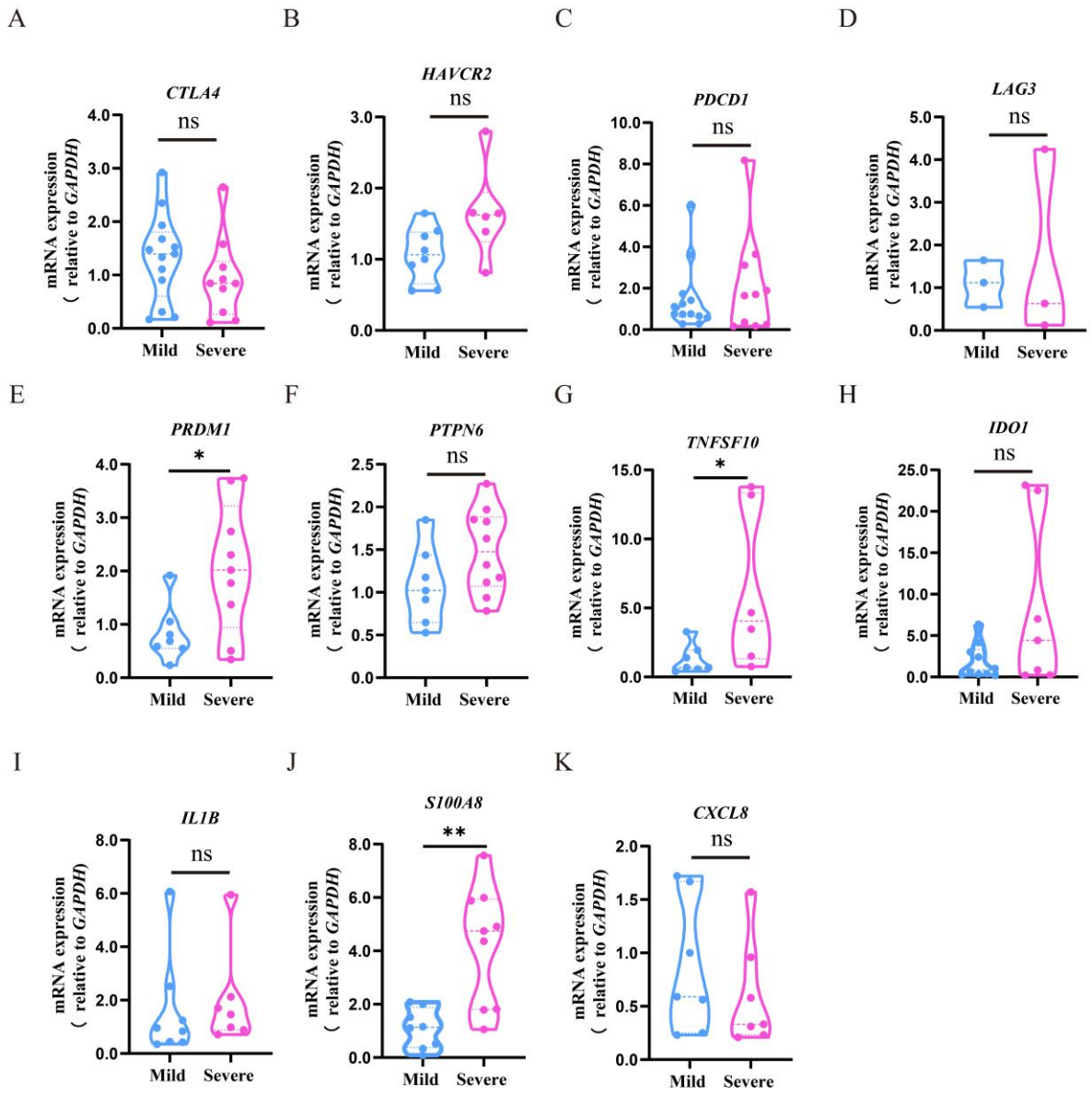


Figure 1. PBMC expression of candidate immune genes in mild and severe MPP. (A) *CTLA4* mRNA expression (Mild n = 13, Severe n = 10); (B) *HAVCR2* mRNA expression (Mild n = 8, Severe n = 6); (C) *PDCD1* mRNA expression (Mild n = 13, Severe n = 10); (D) *LAG3* mRNA expression (Mild n = 3, Severe n = 3); (E) *PRDM1* mRNA expression (Mild n = 8, Severe n = 9); (F) *PTPN6* mRNA expression (Mild n = 7, Severe n = 10); (G) *TNFSF10* mRNA expression (Mild n = 6, Severe n = 7); (H) *IDO1* mRNA expression (Mild n = 10, Severe n = 7); (I) *IL1B* mRNA expression (Mild n = 8, Severe n = 7); (J) *S100A8* mRNA expression (Mild n = 8, Severe n = 9); and (K) *CXCL8* mRNA expression (Mild n = 7, Severe n = 7). Mild: mild group; Severe: severe group. *$P < 0.05$; **$P < 0.01$; ns: not statistically significant.

Subsequent ELISA assays were performed to quantify serum concentrations of protein encoded by the three differentially expressed genes. Serum PRDM1 protein levels were significantly higher in children with SMPP than in the mild subgroup (2270.46 [1929.88, 3107.39] vs. 2111.12 [1713.58, 2494.86] pg/mL, $P < 0.05$). For S100A8, serum concentrations were elevated in both mild and severe MPP subgroups relative to healthy controls ($P < 0.05$). Although SMPP patients showed numerically higher S100A8 levels, no statistically significant difference was identified between the two disease subgroups. Serum TNFSF10 concentration were markedly increased in the mild subgroup compared with healthy controls ($P < 0.05$), while no intergroup difference was found between mild and severe MPP cases (Table 2 and Figure 2).

Considering the significant transcriptional upregulation of PRDM1 and S100A8 in patients with SMPP, together with published evidence indicating that IL-17-mediated inflammation induces pulmonary immune injury during MPP, and this inflammatory cascade further promotes neutrophil secretion of S100A8/A9 and pulmonary epithelial cell apoptosis[25], PRDM1 and S100A8 were retained as candidate variables for subsequent LASSO regression to construct the risk stratification model.

Table 2. Serum Immune Biomarker Protein Levels in the Mild, Severe, and Healthy Control Groups

Biomarker	HC Group	Mild Group	Severe Group
PRDM1 (pg/mL)	1910.08 [1596.18, 2194.57]	2111.12 [1713.58, 2494.86]	2270.46 [1929.88, 3107.39]
S100A8 (pg/mL)	3236.56 [2801.68, 5341.72]	14176.30 [7822.71, 26627.97]	22917.97 [9707.00, 36609.58]
TNFSF10 (pg/mL)	< LOD	4232.03 [2554.69, 4709.53]	2848.53 [252.93, 4293.25]

Note: Values are presented as median [P25, P75] in pg/mL. Sample sizes were as follows: PRDM1: HC group (n = 40), Mild group (n = 154), Severe group (n = 66); S100A8: HC group (n = 35), Mild group (n = 136), Severe group (n = 60); TNFSF10: HC group (n = 7), Mild group (n = 8), Severe group (n = 8). HC, healthy control; LOD, lower limit of detection; <LOD indicates values

below the lower limit of detection of the TNFSF10 assay kit (150 pg/mL).

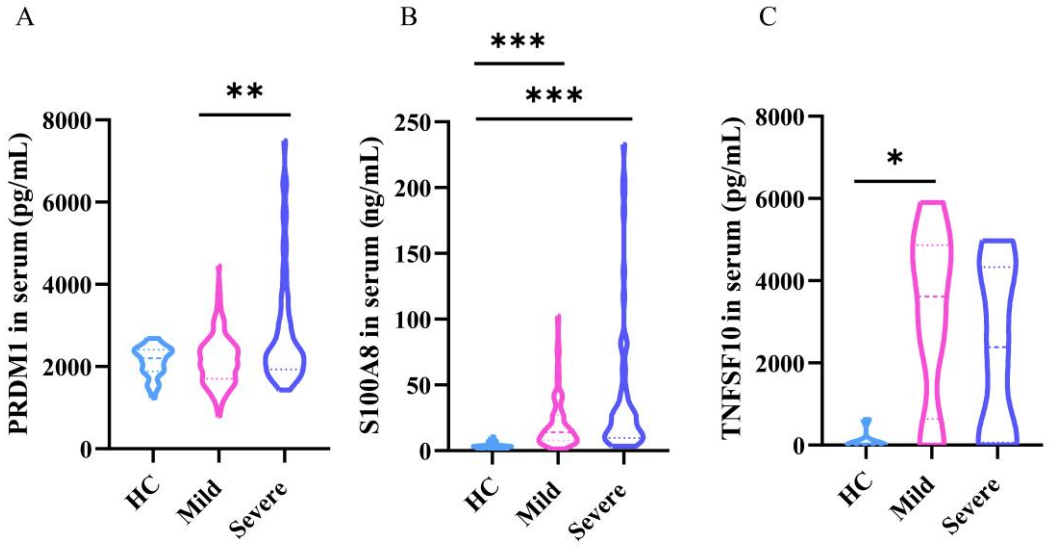


Figure 2. Serum immune biomarker levels across the three study groups. (A) Serum PRDM1 protein level (HC n = 40, Mild n = 154, Severe n = 66); (B) serum S100A8 protein level (HC n = 35, Mild n = 136, Severe n = 60); and (C) serum TNFSF10 protein level (HC n = 7, Mild n = 8, Severe n = 8). HC: healthy control; Mild: mild group; Severe: severe group. *$P < 0.05$; **$P < 0.01$; ***$P < 0.001$.

3.3 LASSO-Logistic Regression Variable Selection

Based on intergroup transcriptional differences, serum quantitative results, and biological functional relevance, PRDM1 and S100A8 were selected as candidate immune biomarkers for constructing the risk stratification model. All candidate variables, including baseline clinical manifestations, routine laboratory parameters, disease severity scoring indices, and the two immune biomarkers, were entered into LASSO-logistic regression with 10-fold cross validation in the training cohort (Figure 3).

The penalty parameter λ was determined according to the cross-validation error curve. λ.min represented the λ value corresponding to the minimum cross validated error, while λ.1se referred to the maximum λ value within one standard error of the minimum error. Thirteen indicators were retained under the λ.min criterion (λ.min = 0.039): wheezing, mPIRO score, PRESS score,

respiratory rate, CRP, hematocrit, red blood cell count, alkaline phosphatase, prealbumin, creatine kinase, LDH, S100A8 and PRDM1. To simplify the model and improve clinical applicability, the more stringent λ.1se criterion (λ.1se = 0.091) was applied for secondary screening, yielding three robust core indicators: PRESS score, LDH and PRDM1. The complete LASSO-logistic regression coefficients under the λ.min and λ.1se criteria are presented in Supplementary Table S7 (Additional file).

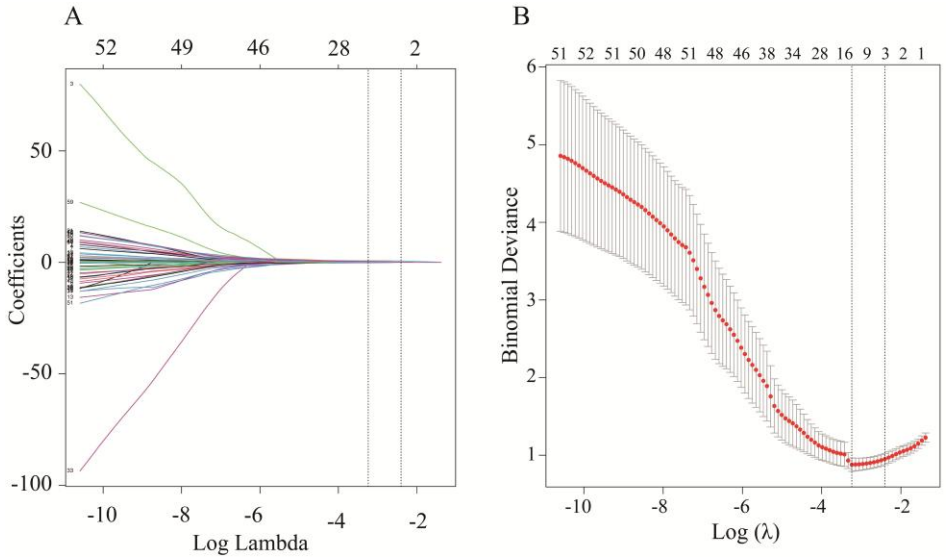


Figure 3. LASSO-logistic regression variable selection results. (A) LASSO coefficient path plot; (B) Cross-validation curve, with dashed lines indicating λ.min and λ.1se.

3.4 Multivariable Logistic Regression Analysis

To further identify independent risk determinants for SMPP and avoid omitting clinically meaningful variables that might be excluded by the stringent λ.1se threshold, all thirteen indicators screened under the λ.min criterion were entered into multivariable logistic regression (Table 3). Four indicators were identified as independent risk determinants of SMPP: PRESS score (OR = 2.960, 95% CI: 1.317–7.566, P = 0.014), LDH (OR = 1.015, 95% CI: 1.005–1.026, P = 0.005), CRP (OR = 1.073, 95% CI: 1.013–1.148, P = 0.022), and serum PRDM1 (OR = 1.001, 95% CI: 1.000–1.002, P = 0.007) (Figure 4).

Table 3. Results of Multivariable Logistic Regression Analysis in the Training Set

Variable	β	SE	OR (95% CI)	Z	*P*
PRESS	**1.085**	**0.442**	**2.960 (1.317–7.566)**	**2.455**	**0.014**
LDH	**0.015**	**0.005**	**1.015 (1.005–1.026)**	**2.814**	**0.005**
CRP	**0.071**	**0.031**	**1.073 (1.013–1.148)**	**2.283**	**0.022**
PRDM1	**0.001**	**< 0.001**	**1.001 (1.000–1.002)**	**2.695**	**0.007**
S100A8	< 0.001	< 0.001	1.000 (1.000–1.000)	1.800	0.072
mPIRO	0.765	0.470	2.148 (0.871–5.632)	1.626	0.104
HCT	−0.106	0.059	0.900 (0.775–1.003)	−1.797	0.072
RR	0.009	0.059	1.009 (0.896–1.132)	0.150	0.881
RBC	−0.718	0.690	0.488 (0.080–1.366)	−1.041	0.298
ALP	−0.007	0.008	0.993 (0.980–1.009)	−0.878	0.380
PAB	−0.006	0.009	0.994 (0.975–1.011)	−0.679	0.497
CK	0.003	0.004	1.003 (0.999–1.011)	0.686	0.493
Wheeze	0.757	0.583	2.131 (0.667–6.749)	1.297	0.195

Note: β, regression coefficient; SE, standard error; OR, odds ratio; CI, confidence interval. Bold entries indicate independent indicators retained in the final model.

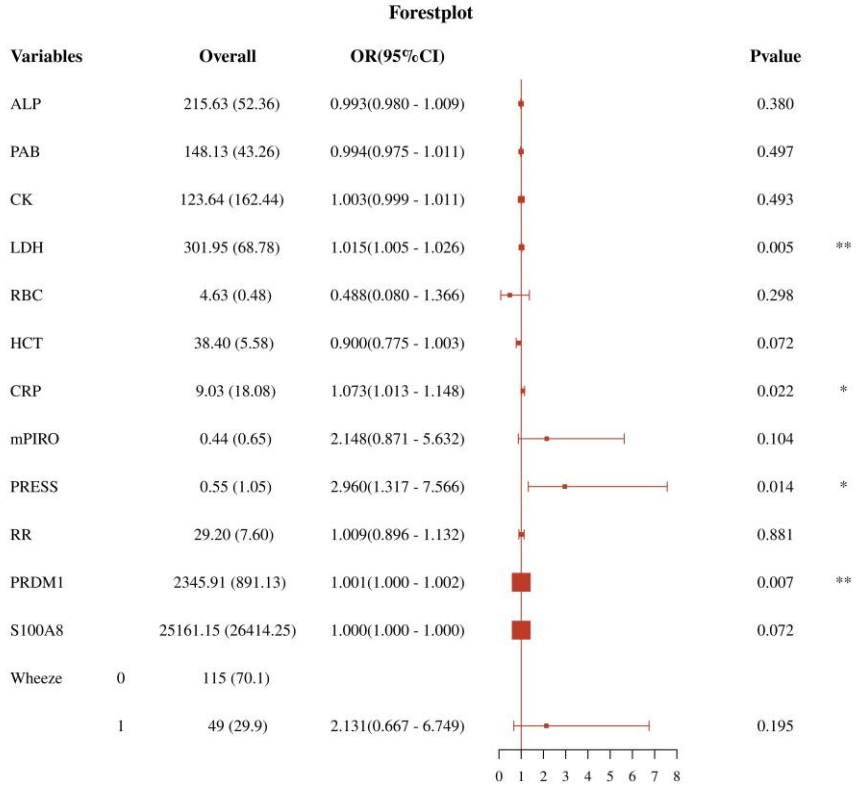


Figure 4. Forest plot of multivariable logistic regression for SMPP-associated variables. LDH:

lactate dehydrogenase; CRP: C-reactive protein; ALP: alkaline phosphatase; PAB: prealbumin; CK: creatine kinase; RBC: red blood cell count; HCT: hematocrit; RR: respiratory rate; PRESS: Pediatric respiratory severity score; mPIRO: modified PIRO score; Wheeze: wheezing.

3.5 Comparison of Three-Variable and Four-Variable Risk Stratification Models

Two candidate risk stratification frameworks were further compared in this study. The three-indicator model comprising PRESS score, LDH and PRDM1 was obtained via the more parsimonious λ.1se screening criterion. The four-indicator model additionally incorporated CRP, which was verified as an independent risk determinant in the foregoing multivariable logistic regression (Table 3 and Figure 4).

In the training cohort, the four-indicator model achieved an AUC of 0.924, compared with 0.897 for the three-indicator model. It also exhibited superior calibration with a lower MAE of 0.050 versus 0.053, and yielded broader clinical net benefit according to decision curve analysis. On the basis of comprehensive performance evaluation, the four-variable model was determined as the final risk stratification nomogram.

3.6 Final Model and Nomogram

The final SMPP risk stratification model for SMPP was constructed based on the four independent risk determinants identified above. The corresponding regression equation is as following:

$$\text{logit}(p) = -8.643 + 0.001 \times \text{PRDM1 (pg/mL)} + 0.082 \times \text{CRP (mg/L)} + 0.015 \times \text{LDH (U/L)} + 1.085 \times \text{PRESS score}$$

The predicted probability of SMPP is calculated using $p = \exp(\eta) / [1 + \exp(\eta)]$. A risk stratification nomogram was established to conveniently quantify individual SMPP risk (Figure 5). Each indicator corresponds to a unique point scale in the nomogram. The total points summed across all indicators can be converted into the corresponding personalized probability of

developing SMPP.

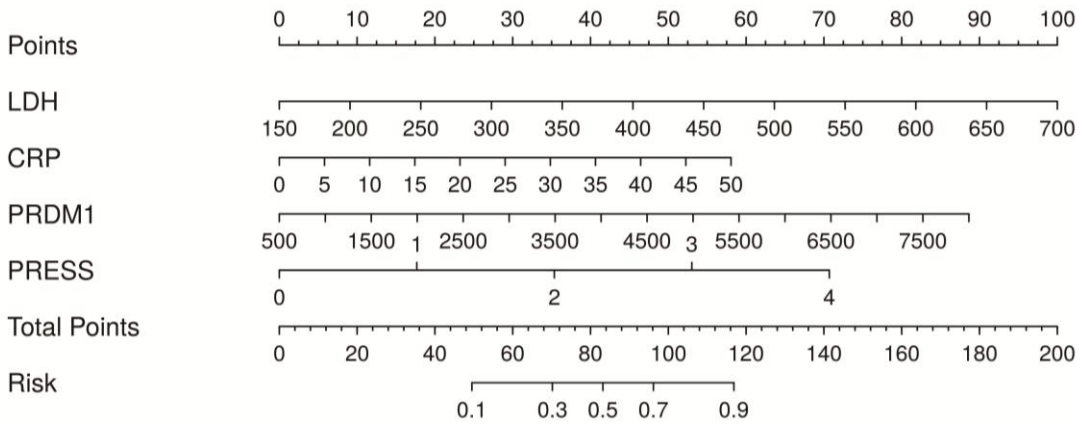


Figure 5. Nomogram for four-variable SMPP risk stratification.

3.7 Discriminative Performance of Single Indicators

ROC analysis was performed to evaluate the standalone discriminatory power of each individual indicator (Table 4, Figure 6). The PRESS score presented the strongest single-indicator discriminative performance, with an AUC of 0.774, sensitivity of 0.633, and specificity of 0.878. LDH yield the second-largest AUC at 0.732. In contrast, PRDM1 and CRP displayed relatively limited standalone discriminatory power, with AUC values of 0.650 and 0.642 respectively. These findings further demonstrate that combining multiple indicators is required to achieve reliable risk stratification.

Table 4. ROC Curve Analysis of Individual Indicators for SMPP (Training Set)

Variable	AUC (95% CI)	Sensitivity	Specificity	Youden Index	Optimal Cutoff
PRESS	0.774 (0.690–0.840)	0.633	0.878	0.511	1.000
LDH	0.732 (0.661–0.825)	0.571	0.861	0.432	327.000
PRDM1	0.650 (0.550–0.737)	0.388	0.861	0.249	2700.798
CRP	0.642 (0.543–0.717)	0.633	0.635	0.267	5.770

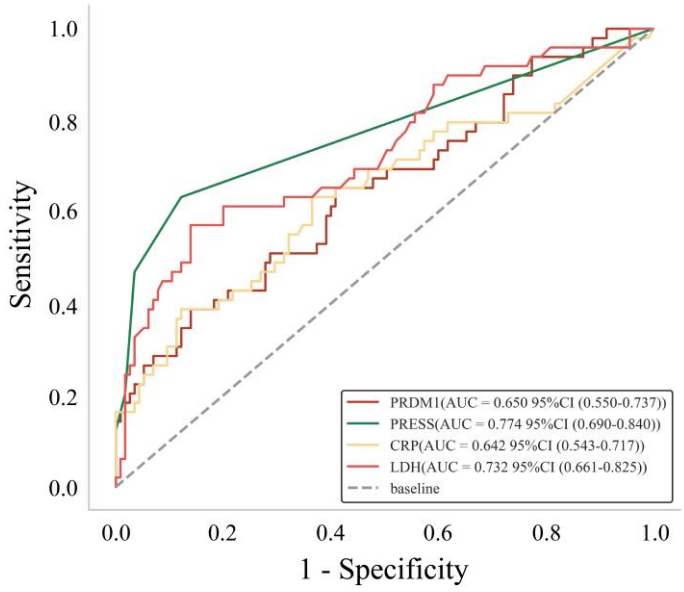


Figure 6. ROC curves for individual indicators (LDH, CRP, PRESS score, PRDM1 protein) in discriminating SMPP.

3.8 Model Discrimination, Calibration, and Clinical Utility

Overall performance of the final four-variable model was assessed in both training and test cohorts for internal validation. The model achieved an AUC of 0.924 (95% CI 0.881–0.967) in the training cohort and an AUC of 0.856 (95% CI 0.751–0.962) in the test cohort, showing acceptable discriminatory power in both subsets (Figure 7B and Figure 8A). Internal calibration was assessed via bootstrap resampling with 1000 replicates. The MAE was 0.050 in the training cohort and 0.036 in the test cohort, reflecting good agreement between model-estimated risk probabilities and actual clinical outcomes (Figures 7D and Figure 8B). Decision curve analysis (DCA) further confirmed the clinical value of this nomogram. Within the threshold probability range of 0.02 to 0.85, the model delivered greater net clinical benefit than two reference strategies (treating all patients or treating none), which supports its clinical applicability (Figure 9).

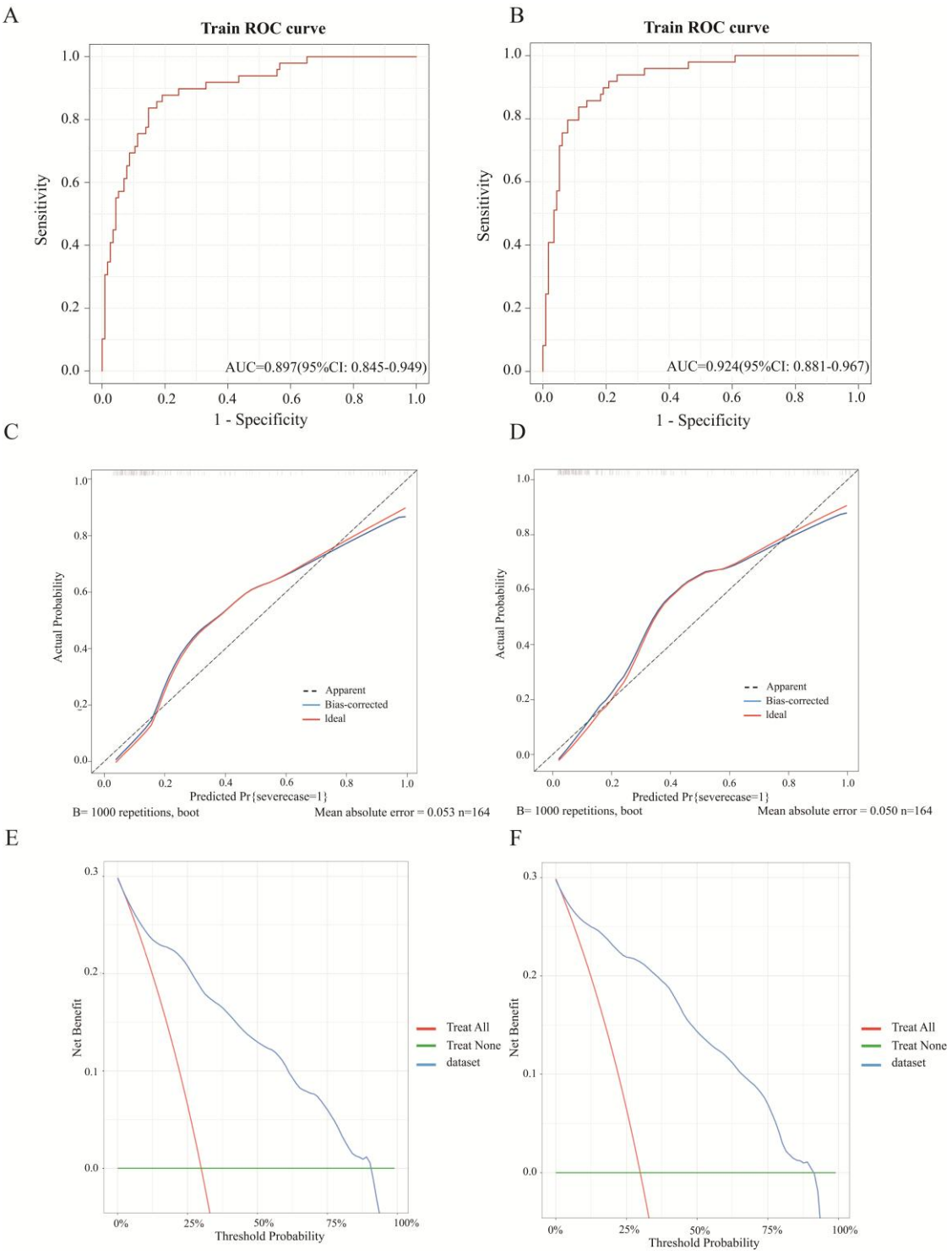


Figure 7. Performance comparison of three- and four-variable models. (A, C, E) Performance of the three-variable model; (B, D, F) performance of the four-variable model. (A–B) ROC curves; (C–D) calibration curves; (E–F) decision curve analysis.

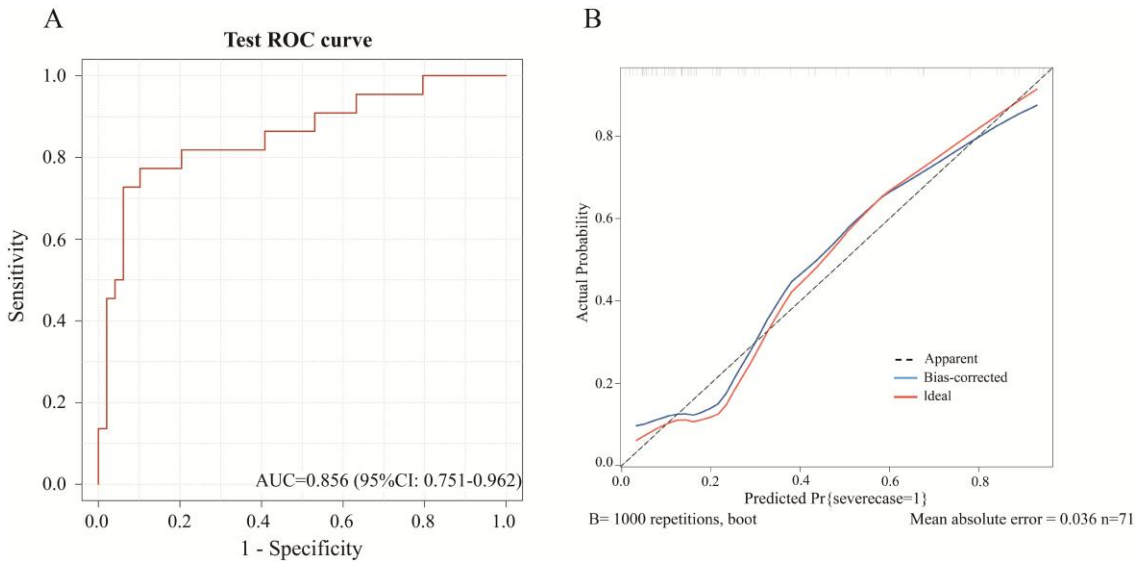


Figure 8. ROC and calibration curves for the four-variable model. (A) Test-set ROC curve (AUC = 0.856; 95% CI: 0.751–0.962); (B) Test-set calibration curve (MAE = 0.036).

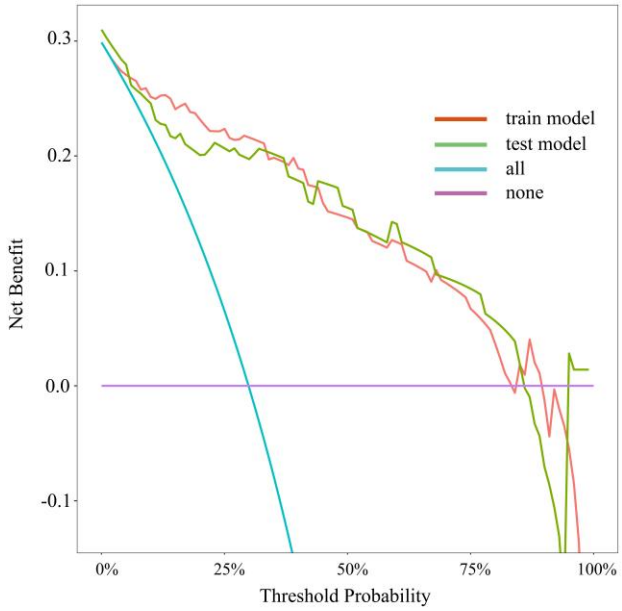


Figure 9. Decision curve analysis (DCA) for the four-variable model.

4. Discussion

This study constructed a risk stratification nomogram for pediatric SMPP by integrating transcriptome-derived immune biomarkers and conventional clinical laboratory parameters. The final model incorporated four independent risk indicators, including the PRESS score, LDH, CRP and serum PRDM1, which collectively reflect respiratory dysfunction, pulmonary tissue injury,

systemic inflammation and peripheral immune imbalance. Internal split-sample validation demonstrated satisfactory discriminative power, with AUC values of 0.924 in the training cohort and 0.856 in the test cohort. The model also exhibited favorable calibration and positive net clinical benefit in DCA, indicating that this concise tool can serve as a reliable auxiliary approach for early identification of children at high SMPP risk in clinical practice.

Among the four selected indicators, LDH, CRP and PRESS score captured distinct clinical manifestations of aggravated MPP. LDH and CRP are widely used markers for tissue damage and systemic inflammation, and their correlation with MPP severity has been validated in previous clinical studies[15, 17]. Consistent with published evidence, both markers were markedly elevated in SMPP patients and confirmed as independent risk factors after multivariate adjustment in our study. LDH acts as a non-specific biomarker of cellular damage; higher LDH levels in the severe group corresponded to more extensive radiological lesions including large pulmonary consolidation, pleural effusion and diffuse patchy infiltrates, further demonstrating aggravated lung tissue injury in children with critical MPP. As a typical acute-phase reactant, CRP quantifies the magnitude of systemic inflammatory cascade. The prominent CRP elevation observed in SMPP patients matched their more severe clinical manifestations, implying a heavier systemic inflammatory burden. As routine, low-cost laboratory tests available at all levels of hospitals, LDH and CRP facilitate the clinical application of this model, especially in primary medical institutions[26].

The PRESS score provides a rapid bedside assessment of respiratory severity by integrating respiratory rate, wheezing, accessory muscle use, peripheral oxygen saturation and feeding status[27]. Its independent risk stratification value aligns with our baseline data showing faster breathing, more frequent wheezing and higher incidence of three-retraction signs among SMPP

children. In contrast, multiple composite peripheral blood inflammatory indices including NLR, PLR, SII and SIRI, which have been reported to correlate with refractory or severe MPP in previous researches[4, 28, 29], exhibited no significant intergroup difference in our cohort. This discrepancy may be attributed to comparable peripheral blood cell counts between non-severe and severe cases, limiting the discriminatory value of these composite indices in our pediatric population. Taken together, these three indicators jointly mirror the three core phenotypic changes of SMPP: lung tissue injury, systemic inflammatory response and progressive respiratory impairment.

The major novelty of the present study lies in the incorporation of the immune regulatory biomarker PRDM1, screened from single-cell transcriptomic profiles, into the SMPP risk stratification system. Accumulating evidence has indicated that pediatric SMPP is driven not only by direct microbial invasion but also by dysregulated host immune-inflammatory responses after MP infection [30]. Given the immature immune status of children, MP infection easily triggers excessive immune activation and persistent inflammatory injury. Single-cell transcriptomic analyses of bronchoalveolar lavage fluid have revealed prominent T cell exhaustion and apoptotic remodeling in the local immune microenvironment of SMPP patients[10, 31]. The PRDM1 gene encodes the transcription factor BLIMP-1, which critically modulates multiple adaptive immune processes, including lymphocyte differentiation, CD8 T cell effector function, T cell exhaustion, and downstream cytokine secretion[32]. In the present study, consistent upregulation of PRDM1 was verified at both the PBMC mRNA and serum protein levels in SMPP children. After adjusting for comprehensive clinical and laboratory covariates, serum PRDM1 remained an independent risk predictor for SMPP. Unlike conventional inflammatory indicators that only reflect superficial tissue damage or systemic inflammation, PRDM1 provides unique adaptive immune signatures,

which effectively complement the conventional indicator system and substantially improve the comprehensive performance of SMPP risk stratification.

In addition, transcriptomic screening detected differential expression of S100A8 and TNFSF10 between MPP severity subgroups, implying that neutrophil-associated inflammatory injury and apoptosis-related immune responses may contribute to pediatric SMPP progression. These results are consistent with previous reports. S100A8/A9 concentrations rise in serum and bronchoalveolar lavage fluid of MPP children and mediate lung injury through the IL-17A-neutrophil-S100A8/A9 axis[25], and serum S100A8/A9 levels correlate with pediatric MPP severity [33]. TNFSF10 encodes the apoptosis-inducing ligand TRAIL, and TRAIL-associated host immune signals have been documented in children with *Mycoplasma pneumoniae*-positive community-acquired pneumonia[34]. PRDM1 and S100A8 both showed upward trends at the transcriptional and serum protein levels. However, only PRDM1 differed significantly between the mild and severe MPP groups and was retained in the final model. Serum S100A8 showed an upward trend in the severe group but was not retained after LASSO selection and multivariable logistic regression. TNFSF10 showed inconsistent transcriptional and protein-level changes and was also excluded from the final model. This mismatch may partly arise from localized pulmonary inflammation, variable disease stages at sampling, or post-transcriptional regulation. These results suggest that peripheral blood S100A8 and TNFSF10 levels cannot stably reflect systemic disease severity in pediatric MPP. In comparison, PRDM1 exhibited consistent upregulation at both mRNA and protein levels, indicating its superior stability as a peripheral immune biomarker for SMPP stratification.

Multiple risk stratification models for pediatric SMPP have been developed based on clinical symptoms, routine laboratory tests and chest imaging results. Most published nomograms adopted

conventional indicators such as age, fever duration, LDH, CRP and pleural effusion, and some models further incorporated complex imaging features or machine learning algorithms to improve performance[4, 35-37]. However, few existing models integrate immune regulatory biomarkers to reflect immune imbalance, a key driver of SMPP deterioration. Relative to previous models, our nomogram only requires four easily accessible variables and achieves moderate discriminatory performance with good interpretability and operability. To our knowledge, this study preliminarily incorporated PRDM1 derived from transcriptomic screening into an SMPP risk stratification nomogram, which can make a modest supplement to the existing indicator system lacking immune molecular markers.

Collectively, our findings demonstrate the potential value of integrating PRDM1 into routine clinical indicators to build a simplified risk stratification tool for pediatric SMPP. Nevertheless, several inherent limitations of this study should be noted when generalizing the conclusions. First, the single-center retrospective enrollment design may introduce inherent selection bias and restrict the external generalizability of the model. Second, only internal split-sample validation was conducted in this research; large-scale multicenter prospective cohorts are required to complete external validation and further optimize the stability of the nomogram. Finally, the exact molecular signaling pathway through which PRDM1 mediates the progression of SMPP remains unclarified, and follow-up cellular and animal functional experiments are warranted to elaborate its regulatory mechanism in MP-induced immune inflammatory disorders.

5. Conclusions

This study screened candidate immune biomarkers for pediatric SMPP based on single-cell transcriptomic data. Transcriptional upregulation of PRDM1, S100A8 and TNFSF10 was observed in children with SMPP, suggesting the participation of immune and inflammatory

pathways in disease aggravation. However, only PRDM1 presented consistent elevated expression at both peripheral blood mRNA and serum protein levels, and was confirmed as an independent risk determinant for severe MPP. We established a concise four-variable risk stratification nomogram integrating PRDM1, LDH, CRP and PRESS score. Internal validation verified its reliable discrimination, acceptable calibration and favorable clinical net benefit. This simple, readily accessible model could act as an auxiliary tool for early risk assessment and stratified management of pediatric SMPP in clinical practice.

List of abbreviations

AUC: Area under the receiver operating characteristic curve

BALF: Bronchoalveolar lavage fluid

CI: Confidence interval

CRP: C-reactive protein

DCA: Decision curve analysis

ELISA: Enzyme-linked immunosorbent assay

HC: Healthy control

IQR: Interquartile range

LASSO: Least absolute shrinkage and selection operator

LDH: Lactate dehydrogenase

LOD: Limit of detection

MAE: Mean absolute error

MPP: *Mycoplasma pneumoniae* pneumonia

mPIRO: Modified predisposition, insult, response, and organ dysfunction score

OR: Odds ratio

PBMCs: Peripheral blood mononuclear cells

PRDM1: PR/SET domain 1

PRESS: Pediatric Respiratory Severity Score

ROC: Receiver operating characteristic

RT-qPCR: Reverse transcription quantitative polymerase chain reaction

S100A8: S100 calcium-binding protein A8

scRNA-seq: Single-cell RNA sequencing

SMPP: Severe Mycoplasma pneumoniae pneumonia

TNFSF10: Tumor necrosis factor superfamily member 10

Declarations

Clinical trial number

Not applicable.

Ethics approval and consent to participate

This study was carried out in strict accordance with the ethical principles laid down in the Declaration of Helsinki. The protocol was approved by the Ethics Committee of Zunyi First People's Hospital on September 6, 2023 (Approval No. Ethics Review [2023]-1-271). Written informed consent was signed and provided by the parents or legal guardians of all enrolled participants.

Consent for publication

Not applicable.

Availability of data and materials

The datasets generated and/or analyzed during the current study are not publicly available due to privacy and ethical restrictions, but are available from the corresponding author on reasonable request.

Competing interests

The authors declare that they have no competing interests.

Funding

The research was financially supported by National Natural Science Foundation of China (Grant Nos. 82560398 and 82500045), Guizhou High-level (BAI) Innovative Talents Project (QIANKehe Platform & Talents-GCC [2022]042-1), 2025 National Key Clinical Specialty Construction Project (Clinical Laboratory), and the Funds of the Guizhou Provincial Health Commission Clinical Key Specialty Construction "Peak Climbing Plan" Project (No. GZWJWPF2025021).

Authors' contributions

MJ contributed to the conceptualization and design of the study, clinical data collection, experimental investigation, data analysis, and preparation of the original manuscript. AW, JD and YA contributed to clinical data collection and data curation. TL and LL contributed to experimental investigation and sample processing. KW and SY contributed to supervision, project administration, funding acquisition, and writing—review and editing. All authors read and approved the final manuscript.

Acknowledgements

Not applicable.

Additional files

File format: Microsoft Word document (.docx)

Title of data: Supplementary Tables S1–S7

Description of data: Supplementary Table S1 presents the primer sequences used for RT-qPCR. Supplementary Tables S2–S6 present complete comparisons of clinical characteristics and physical signs, imaging findings, complete blood count parameters, biochemical indicators, inflammatory indicators, and severity scores between the mild and severe MPP groups. Supplementary Table S7 presents the LASSO-logistic regression coefficients under the λ.min and λ.1se criteria.

References

1. The Subspecialty Group of Respiratory, the Society of Pediatrics, Chinese Medical Association, China National Clinical Research Center of Respiratory Diseases, Editorial Board, Chinese Journal of Pediatrics. Evidence-based guideline for the diagnosis and treatment of Mycoplasma pneumoniae pneumonia in children (2023). Pediatr Investig. 2025;9(1):1–11.
2. Lind K, Benzon MW, Jensen JS, Clyde WA, Jr. A seroepidemiological study of Mycoplasma pneumoniae infections in Denmark over the 50-year period 1946-1995. Eur J Epidemiol. 1997;13(5):581–6.
3. Diaz MH, Hersh AL, Olson J, Shah SS, Hall M, Edens C. Mycoplasma pneumoniae Infections in Hospitalized Children - United States, 2018-2024. MMWR Morb Mortal Wkly Rep. 2025;74(23):394–400.
4. Zhang X, Sun R, Jia W, Li P, Song C. A new dynamic nomogram for predicting the risk of severe Mycoplasma pneumoniae pneumonia in children. Sci Rep. 2024;14:8260.
5. Meyer Sauteur PM, Beeton ML, European Society of Clinical Microbiology and Infectious Diseases (ESCMID) Study Group for Mycoplasma and Chlamydia Infections (ESGMAC), and the ESGMAC Mycoplasma pneumoniae Surveillance (MAPS) study group. Mycoplasma pneumoniae: delayed re-emergence after COVID-19 pandemic restrictions. Lancet Microbe. 2024;5(2):e100–e1.
6. Zhao X, Lv J, Wu M, Wu Q. Clinical characteristics and risk factors for Mycoplasma pneumoniae pneumonia in children. Front Pediatr. 2024;12:1438631.
7. Miglioretti DL, Johnson E, Williams A, Greenlee RT, Weinmann S, Solberg LI, et al. The use of computed tomography in pediatrics and the associated radiation exposure and estimated cancer risk. JAMA Pediatr. 2013;167(8):700–7.
8. Pearce MS, Salotti JA, Little MP, McHugh K, Lee C, Kim KP, et al. Radiation exposure from

CT scans in childhood and subsequent risk of leukaemia and brain tumours: a retrospective cohort study. Lancet. 2012;380(9840):499–505.
9. Zhu Y, Luo Y, Li L, Jiang X, Du Y, Wang J, et al. Immune response plays a role in Mycoplasma pneumoniae pneumonia. Front Immunol. 2023;14:1189647.
10. Shen X, Jin Z, Chen X, Wang Z, Yi L, Ou Y, et al. Single-cell transcriptome atlas revealed bronchoalveolar immune features related to disease severity in pediatric Mycoplasma pneumoniae pneumonia. MedComm (2020). 2024;5(10):e748.
11. Zhang Z, Dou H, Tu P, Shi D, Wei R, Wan R, et al. Serum cytokine profiling reveals different immune response patterns during general and severe Mycoplasma pneumoniae pneumonia. Front Immunol. 2022;13:1088725.
12. Jiang C, Bao S, Shen W, Wang C. Predictive value of immune-related parameters in severe Mycoplasma pneumoniae pneumonia in children. Transl Pediatr. 2024;13(9):1521–8.
13. Yang M, Meng F, Wang K, Gao M, Lu R, Li M, et al. Interleukin 17A as a good predictor of the severity of Mycoplasma pneumoniae pneumonia in children. Sci Rep. 2017;7:12934.
14. Yang M, Meng F, Gao M, Cheng G, Wang X. Cytokine signatures associate with disease severity in children with Mycoplasma pneumoniae pneumonia. Sci Rep. 2019;9(1):17853.
15. Liu F, Chen L, Wang MY, Shi WJ, Wang XP. Exploring high-risk factors for the prediction of severe mycoplasma pneumonia in children. Transl Pediatr. 2024;13(11):2003–11.
16. Bi Y, Zhu Y, Ma X, Xu J, Guo Y, Huang T, et al. Development of a scale for early prediction of refractory Mycoplasma pneumoniae pneumonia in hospitalized children. Sci Rep. 2021;11(1):6595.
17. Shen F, Dong C, Zhang T, Yu C, Jiang K, Xu Y, et al. Development of a Nomogram for Predicting Refractory Mycoplasma pneumoniae Pneumonia in Children. Front Pediatr. 2022;10:813614.
18. Valentania V, Somasetia DH, Hilmanto D, Setiabudi D, Nataprawira HMN. Modified PIRO (predisposition, insult, response, organ dysfunction) severity score as a predictor for mortality of children with pneumonia in Hasan Sadikin Hospital, Bandung, Indonesia. Multidiscip Respir Med. 2021;16(1):735.
19. Kanwal N, Shahzad M, Rehman A, Haq AU, Khalid R, Ghazanfar S, et al. Evaluation of Bronchiolitis Severity and Hospitalization Rates in Pediatric Patients in Developing Countries Using the Pediatric Respiratory Severity Score. Cureus. 2025;17(3):e81173.
20. Stekhoven DJ, Bühlmann P. MissForest--non-parametric missing value imputation for mixed-type data. Bioinformatics. 2012;28(1):112–8.
21. Friedman J, Hastie T, Tibshirani R. Regularization Paths for Generalized Linear Models via Coordinate Descent. J Stat Softw. 2010;33(1):1–22.
22. Hanley JA, McNeil BJ. The meaning and use of the area under a receiver operating characteristic (ROC) curve. Radiology. 1982;143(1):29–36.
23. Austin PC, Steyerberg EW. The Integrated Calibration Index (ICI) and related metrics for quantifying the calibration of logistic regression models. Stat Med. 2019;38(21):4051–65.
24. Vickers AJ, Elkin EB. Decision curve analysis: a novel method for evaluating prediction models. Med Decis Making. 2006;26(6):565–74.
25. Bai S, Wang W, Ye L, Fang L, Dong T, Zhang R, et al. IL-17 stimulates neutrophils to release S100A8/A9 to promote lung epithelial cell apoptosis in Mycoplasma pneumoniae-induced pneumonia in children. Biomed Pharmacother. 2021;143:112184.
26. Luo Y, Wang Y. Risk Prediction Model for Necrotizing Pneumonia in Children with Mycoplasma pneumoniae Pneumonia. J Inflamm Res. 2023;16:2079–87.

27. Jagalamarri VL, Balleda L, Kolla S, Chandra Sekhara Reddy T. Utility of PRESS Score in Predicting the Outcomes of Children Admitted with Respiratory Distress: A Prospective Study. Pediatric Respirology and Critical Care Medicine. 2021;5(4):57–61.
28. Wang S, Wan Y, Zhang W. The Clinical Value of Systemic Immune Inflammation Index (SII) in Predicting the Severity of Hospitalized Children with Mycoplasma Pneumoniae Pneumonia: A Retrospective Study. Int J Gen Med. 2024;17:935–42.
29. Guo X, Luo H, Song Y, Xiao L, Xu X, Guo Y. Application value of systemic immune-inflammation index in predicting severe Mycoplasma pneumoniae pneumonia. PLoS One. 2025;20(10):e0333267.
30. Shi S, Zhang X, Zhou Y, Tang H, Zhao D, Liu F. Immunosuppression Reduces Lung Injury Caused by Mycoplasma pneumoniae Infection. Sci Rep. 2019;9(1):7147.
31. Chen X, Liu F, Zheng B, Kang X, Wang X, Mou W, et al. Exhausted and Apoptotic BALF T Cells in Proinflammatory Airway Milieu at Acute Phase of Severe Mycoplasma Pneumoniae Pneumonia in Children. Front Immunol. 2022;12:760488.
32. Shin H, Blackburn SD, Intlekofer AM, Kao C, Angelosanto JM, Reiner SL, et al. A role for the transcriptional repressor Blimp-1 in CD8(+) T cell exhaustion during chronic viral infection. Immunity. 2009;31(2):309–20.
33. Zhou P, Peng L, Xu L, Liu QH, Huang H, Zhong LL. [Value of calprotectin S100 A8/A9 in predicting the severity of Mycoplasma pneumoniae pneumonia in children]. Zhongguo Dang Dai Er Ke Za Zhi. 2024;26(7):716–22.
34. Papan C, Sidorov S, Greiter B, Bühler N, Berger C, Becker SL, et al. Combinatorial Host-Response Biomarker Signature (BV Score) and Its Subanalytes TRAIL, IP-10, and C-Reactive Protein in Children With Mycoplasma pneumoniae Community-Acquired Pneumonia. J Infect Dis. 2024;230(2):e247–e53.
35. Liu S, Zhang L, Dai L, Li J, Li D. Prediction model for severe mycoplasma pneumoniae pneumonia and analysis of macrolide-resistance in children: a case-control study. Ital J Pediatr. 2025;51:180.
36. Xie S, Wu M, Shang Y, Tuo W, Wang J, Cai Q, et al. Development and validation of an early diagnosis model for severe mycoplasma pneumonia in children based on interpretable machine learning. Respir Res. 2025;26(1):182.
37. Li L, Guo R, Zou Y, Wang X, Wang Y, Zhang S, et al. Construction and Validation of a Nomogram Model to Predict the Severity of Mycoplasma pneumoniae Pneumonia in Children. J Inflamm Res. 2024;17:1183–91.

Supplementary Files

This is a list of supplementary files associated with this preprint. Click to download.

- Additionalfile.docx